Journal of Groundwater Science and Engineering
ISSN 2305-7068
Indexed by ESCI CABI CSA
Scopus GeoRef AJ CNKI

Using pore-solid fractal dimension to estimate residual LNAPLs saturation in sandy aquifers: A column experiment

Lin Sun, Shuai-wei Wang, Cai-juan Guo, Chan Shi, Wei-chao Su

Citation:
Sun L, Wang SW, Guo CJ, *et al*. 2022. Using pore-solid fractal dimension to estimate residual LNAPLs saturation in sandy aquifers: A column experiment. Journal of Groundwater Science and Engineering, 10(1): 87-98.

View online: https://doi.org/10.19637/j.cnki.2305-7068.2022.01.008

Journal homepage: http://gwse.iheg.org.cn

Using pore-solid fractal dimension to estimate residual LNAPLs saturation in sandy aquifers: A column experiment

Lin Sun[1,2], Shuai-wei Wang[1,2*], Cai-juan Guo[1], Chan Shi[1], Wei-chao Su[1]

[1] *Institute of Hydrogeology and Environmental Geology*, *Chinese Academy of Geological Sciences Resources*, *Shijiazhuang* 050061, *China*.
[2] *Key Laboratory of Groundwater Sciences and Engineering*, *Ministry of Natural*, *Shijiazhuang* 050061, *China*.

Abstract: : The"tailing" effect caused by residual non-aqueous phase liquids (NAPLs) in porous aquifers is one of the frontiers in pollution hydrogeology research. Based on the current knowledge that the residual NAPLs is mainly controlled by the pore structure of soil, this study established a method for evaluating the residual saturation of NAPLs by investigating the fractal dimension of porous media. In this study, the soil column experiments of residual light NAPLs (LNAPLs) in sandy aquifer with different ratios of sands and soil were carried out, and the correlation between the fractal dimension of the medium, the residual of LNAPLs and the soil structure parameters are statistically analyzed, and its formation mechanism and main control factors are discussed. The results show that: Under our experimental condition: (1) the fractal dimension of the medium has a positive correlation with the residual saturation of NAPLs generally, and the optimal fitting function can be described by a quadratic model: $S_R = 192.02D^2 - 890.73D + 1\,040.8$; (2) the dominant formation mechanism is: Smaller pores in the medium is related to larger fractal dimension, which leads to higher residual saturation of NAPLs; stronger heterogeneity of the medium is related to larger fractal dimension, which also leads to higher residual saturation of NAPLs; (3) the micro capillary pores characterized by fine sand are the main controlling factors of the formation mechanism. It is concluded that both the theory and the method of using fractal dimension of the medium to evaluate the residual saturation of NAPLs are feasible. This study provides a new perspective for the research of "tailing" effect of NAPLs in porous media aquifer.

Keywords: Residual saturation; NAPLs; Pore structure; Fractal; Tailing effect

Received: 12 Apr 2021/ Accepted: 19 Jan 2022

Introduction

Non-aqueous phase liquids (NAPLs) can be divided into two categories: Light non-aqueous phase liquids (LNAPLs) and dense non-aqueous phase liquids (DNAPLs) according to the relationship with water density. The "tailing" effect in the process of NAPLs pollution remediation in porous media is hotspot and difficult issue internationally (Mackay & Cherry, 1989; Gao et al. 2008; Wang et al. 2016; Mateas et al. 2017; Zhao et al. 2018; Ezeh, 2019; Rane et al. 2020; Ramezanzadeh et al. 2020; Cheng & Zhu, 2021). Previous studies have shown (Hunt et al. 1988; Mackay et al. 1991; Forsyth PA & Shao, 1991) that "tailing" is mainly due to the fact that NAPLs are intercepted by some pores and become an independent residual phase, which is difficult to be removed by external force. The ratio of its pore volume to the total pore volume is called residual saturation (Fetter et al. 1999) (Fig. 1), where (a) represents NAPLs in a continuous free phase, and (b) stands for NAPL droplets in the independent residual phase. The level of residual saturation has little to do with the chemical properties of NAPLs (Saripalli et al. 1998). It is mainly related to the structure and composition of the soil, and largely depends on the geometry of the capillary pores that can completely bind the NALPs, such as the connectivity, size and porosity of pores.

As early as 1999, Wiedemeier summarized and proposed a multiphase flow model from the field scale of 100 meters to the capillary scale of millimeter or even smaller scales to describe NAPLs,

*Corresponding author: Shuai-wei Wang, *E-mail address*: Tairan_W@163.com

DOI: 10.19637/j.cnki.2305-7068.2022.01.008

Sun L, Wang SW, Guo CJ, et al. 2022. Using pore-solid fractal dimension to estimate residual LNAPLs saturation in sandy aquifers: A column experiment. Journal of Groundwater Science and Engineering, 10(1): 87-98.

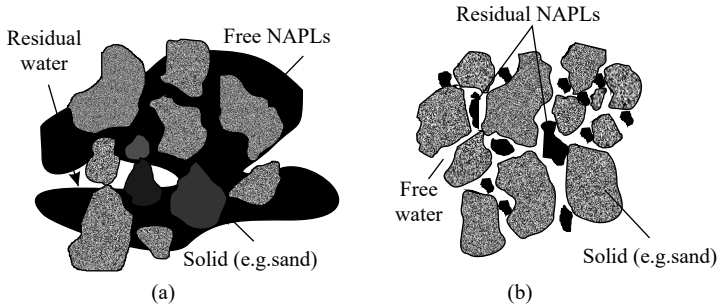

Fig. 1 Occurrence status of NAPLs in aquifers

and this method is currently the main method for studying NAPLs. This series of models generally requires parameters such as capillary pressure, saturation, relative permeability, surface tension and wettability. Theoretically, the residual saturation can be calculated by determining these parameters.

However, in practical work, most parameters can only be obtained through indoor water-soil-NAPLs simulation experiment (Celia et al. 1995; White et al. 2004; Zhang & Kang, 2007; Hou et al. 2019; Karaoglu et al. 2019; Kacem et al. 2019; Khasi et al. 2020), which requires rigorous test scheme and precise instruments and equipment to ensure the accuracy of the experiment. Moreover, the measurements of capillary pressure, saturation and its lag effect have always been difficult. Even if the simulation test results are reliable, the difference of scale effect between laboratory and field is hard to avoid.

In order to solve many complex problems of multiphase flow model parameters, some researchers have introduced fractal theory to study NAPLs (Kemblowski & Wen, 1993; Neuman, 1995; Yu, 2003; Feng et al. 2019; Soto et al. 2019). A few researchers tried to describe the migration process of NAPLs with phase parameters-fractal (dimension and scale) (Mukhopadhyay & Cushman, 1998; Costa, 2006; Li et al. 2013; Patmonoaji et al. 2020). Probably because these studies are lack of in-depth disclosure of the mechanism, the fractal methods are not widely accepted, and have not been used to characterize the residual saturation of NAPLs. However, according to the definition of NAPLs residual saturation and its occurrence form in porous aquifers, the microscopic pore characteristics of the medium are the key factors in determining the residual saturation of NAPLs. The multiphase flow parameters (relative permeability, capillary pressure, saturation etc.) are essentially the macroscopic representations of the microscopic pore characteristics of the medium. Therefore, it is reasonable and feasible to estimate the residual saturation of NAPLs as long as the microscopic pore structure of the medium can be accurately characterized.

In fact, many studies on fractal characterization of residual oil distribution and residual saturation have been carried out in the field of petroleum geology (Jia et al. 1995; Le & Wang, 2004; Li et al. 2006; Yang & Xu, 2009; Zhang & Ren, 2011; Zhang et al. 2013; Guo et al. 2014; Liu et al. 2017; Han et al. 2018), and these studies were mainly conducted in glutenite debris media. The research shows that the fractal dimension of the rock debris medium is positively correlated with the residual saturation, and the formation is related to the heterogeneity. Based on this, it is inferred that the NAPLs residues in the soil medium should also have fractal characteristics.

Based on the above analysis, in this study, quartz sand was used to mix soil with different pore structure characteristics, and the common light non-aqueous phase liquid (LNAPLs) material, diesel, was used to carry out the LNAPLs residual soil column simulation experiments. A method is therefore proposed for estimating the residual saturation of LNAPLs by the fractal dimension of the medium to provide support for the remediation of LNAPLs pollution in sandy aquifers.

1 Materials and methods

1.1 Materials

Main materials: LNAPLs: 0# diesel with a density of 0.83 g/ml; quartz sand (3 kinds): Fine grain (212 μm), medium grain (380 μm) and coarse grain (830 μm) (Table 4).

Main instruments: Emulsifier, digestion apparatus, portable spectrophotometer, laser particle size analyzer, oven, scale, etc.

Soil column setup: The soil column is 1 meter high with the inner diameter of 6cm, and thickness of 0.5 cm. The water inlet is set at a distance of about 10 cm from the upper end of the column, which is connected to the constant head device, and the head measuring device is connected to the position of 15 cm from the upper end and 5 cm from the lower end in the column (Fig. 2).

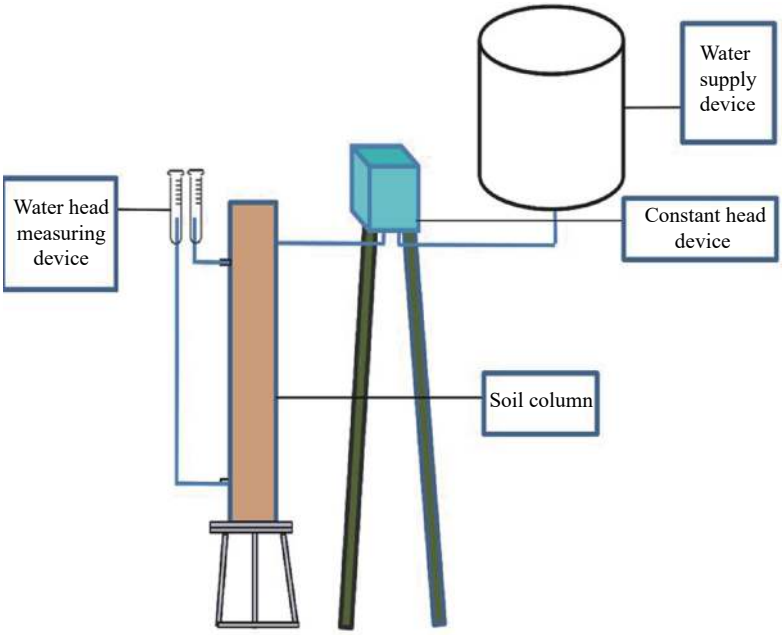

Fig. 2 Schematic diagram of soil column simulation test device

1.2 Soil column simulation experiment

In order to reduce the volatilization of diesel during the experiment, the experiment was conducted in winter. The soil column, the baseplate, the constant water head device and the water supply bucket are connected with a latex tube, and a gauze was placed at the bottom of the soil column to prevent the quartz sand from flowing out with the water. The experiment mainly includes two processes: The preparation of sandy aquifer and formation of LNAPLs residual.

1.2.1 Preparation of sandy aquifer

The fine, medium and coarse quartz sands were randomly mixed into four configurations with different particle ratios of T1, T2, T3 and T4 (Table 4). Each configuration had two repetitions, so there were eight experimental soil columns identified as 1-1, 1-2, 2-1, 2-2, 3-1, 3-2, 4-1 and 4-2 (Table 1) respectively. The specific proportioning details are shown in Table 4.

Table 1 Particle ratio scheme of soil column medium

Treatment	T1		T2		T3		T4	
NO.	1-1	1-2	2-1	2-2	3-1	3-2	4-1	4-2

Before the filling experiment started, the water inlet pipe was connected to the water outlet below the soil column, then water was injected from the bottom of the device until the water surface just reached the connection level between the flange and the column, and started to add samples. The total filling volume was about 9 600 cm^3, which was divided into 8 times. The height and quality of sand samples in each soil column were the same. During the filling, the column wall was patted gently to make sure it was properly filled. Water injection rate was carefully controlled after each filling. Water injection was stopped when the quartz sand was fully soaked in water and the next filling started. Filling was stopped when the sample height in the column reached about 85 cm. After the filling was completed, the water inlet was move to the upper end of the soil column, and water was injected into each soil column. The water levels in the eight columns were consistent with each other and a hydraulic gradient was kept between 0.01-0.03. The flow rate was monitored for 12 times in about 16 hours. The permeability coefficient did not change much (within a relative error of 30%) and it was considered that the medium structure was stable, and the preparation of the sand medium aquifer was completed.

1.2.2 Formation of LNAPLs residual

After the water injection stopped, 500 mL of diesel was added to the soil column. When the soil surface just reached the top of the quartz sand, the water pipe of the water inlet device was connected to the sandbox and the water levels in all soil columns were kept the same. The flowing out volume of oil and water was recorded, and samples were taken. COD_{Cr} was taken as the quantitative indicator of diesel concentration, which was measured in the sample. When the COD_{Cr} value of the effluent samples in each soil column was 0, we considered that the diesel had completely flowed out with the relative error of the permeability coefficient within 30%. At this stage, it was

considered that the residual NAPLs had formed, and the soil height in each soil column was measured to calculate the soil volume. The experiment was over.

1.3 Data analysis

1.3.1 Residual saturation of LNAPLs

Since the outflow was a heterogeneous mixture of oil and water, to obtain accurate and representative data an emulsifying machine was used to mix the oil and water uniformly, and samples were then taken to measure COD_{Cr}. The scatter plot of the concentrations of NAPLs and COD_{Cr} shows a very strong linear relationship with R^2 of 0.999 1 (Fig. 3).

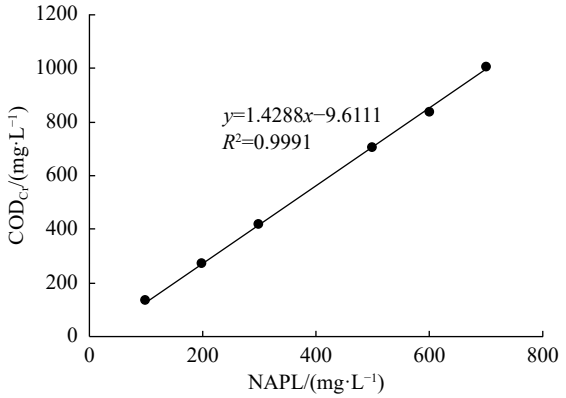

Fig. 3 Scatter plot of NAPLs-CODcr

The operation processes are as follows: (1) configure 500 mL of oil and water with six concentration levels of 100, 200, 300, 500, 600, and 700 mg/L; (2) set the emulsifier speed at 5 500 r/min, and emulsify each of water-oil samples for 3 minutes from low to high concentration; (3) use a pipette to take up 2 mL of the solution, and put it in a HACH special COD_{Cr} test tube with potassium dichromate as an indicator; (4) digest the solution with a digester for 2 hours, then take out the test tube and cool it; (5) measure the COD_{Cr} of the sample on a portable UV spectrophotometer.

By this way, the amount of total LNAPLs in the effluent flowing out the soil column can be determined. The residual amount of LNAPLs in the soil column can be calculated by subtracting the amount of oil flowing out from the total amount of oil added, denoted as V_{soil}. The residual saturation can then be determined as:

$$S_R\% = \frac{V_{soil}}{V_{soil} - V_{sand}} \times 100 \quad (1)$$

Where: V_{soil} is the residual oil volume, V_{soil} is the soil volume, V_{sand} is the sand volume, and S_R is the residual saturation.

1.3.2 Fractal dimension of sand medium

After the experiment, the sand samples in the soil columns were randomly taken, washed and dried to record the quality. The laser particle size analyzer Mastersizer-2000 was used to measure and count the mass distribution of different particle size, i.e. 0.03-0.3 mm, 0.3-0.4 mm, 0.4-0.5 mm, 0.5-0.65 mm, 0.65-0.8 mm, 0.8-1 mm, 1-2 mm. The density of the soil with the same particle size is largely the same, and the commonly used Yang Peiling method can be applied to calculate the fractal dimension of the soil. The calculation formula is:

$$\left(\frac{\overline{R_i}}{R_{\max}}\right)^{3-D} = \frac{W\left(d < \overline{R_i}\right)}{W_0} \quad (2)$$

Where: R_i is the i-th particle size in the particle, $\overline{R_i}$ represents the average particle size between the two sieve grades R_i and R_{i+1}, abbreviated as R_i; R_{max} is the average largest particle size, abbreviated as R_{max}; $W(d < R_i)$ represents the cumulative weight of particles smaller than R_i, abbreviated as $\frac{W}{W_0}$; W_0 represents the total weight of particles.

The formula can be simplified into:

$$\lg\frac{W}{W_0} = (3-D)\lg\frac{R_i}{R_{\max}} \Rightarrow \mathrm{D} = 3 - \frac{\lg(\mathrm{W}/W_0)}{\lg(R_i/R_{\max})} \quad (3)$$

Take $\lg\frac{W}{W_0}$ as the ordinate and $\lg\frac{R_i}{R_{\max}}$ as the abscissa to make a log-log plot to describe the particle size distribution, the relationship can be fitted with a straight line and the slope of the line is $3-D$, from which the fractal dimension D can be calculated.

1.3.3 Other parameters

The initial porosity of the soil is calculated by:

$$n_0\% = \frac{V_{soil} - V_{sand}}{V_{soil}} \times 100 \quad (4)$$

Where: V_{soil} is the volume of soil, V_{sand} is the volume of sand, and n_0 is the initial porosity.

The permeability coefficient is calculated by Darcy's law, the details of which are not given in this paper.

2 Results and discussion

2.1 Data presentation

The first three permeability coefficient before the formation of LNAPLs residues were calculated using Darcy' s law, ranging from 27.35 m/d to 79.16 m/d, and the relative error RSD is between 1% and 27%, as shown in Table 2.

Table 2 the observed results of the three permeability coefficients before the end of the residual LNAPLs formation experiment

	1-1	1-2	2-1	2-2	3-1	3-2	4-1	4-2
Third from last	80.08	54.05	39.8	53.72	27.75	51.68	37.88	40.58
Second from last	79.83	41.84	40.37	66.06	27.3	31.2	36.23	45.89
Last	77.58	56.65	45.55	64.3	26.99	36.57	37.01	53.05
RSD%	6	16	8	11	1	27	2	13

The above experimental methods were used to measure the volume of soil, sand, residual oil and soil particle mass, and the cumulative soil particle weight data for the 7 grades (0.03-0.3 mm、0.3-0.4 mm、0.4-0.5 mm、0.5-0.65 mm、0.65-0.8 mm、0.8-1 mm、1-2 mm), the results are shown in Table 3.

The residual saturation and initial porosity are calculated by:

$$S_R\% = \frac{V_{soil}}{V_{soil} - V_{sand}} \times 100 \quad (5)$$

$$n_0\% = \frac{V_{soil} - V_{sand}}{V_{soil}} \times 100 \quad (6)$$

The fractal dimension is calculated by Yang Peiling method. In order to make the calculation more accurate, use two line segments with 3 points each (Line 1 and Line 2) to fit the data, R^2 was above 0.95 for all samples. After the fractal dimension was calculated for each section, the mean value was taken to represent the fractal dimension of the entire soil (Fig. 4, Table 4).

Where: SD is the standard error, Average is the mean value.

2.2 Results

2.2.1 Relationship between residual saturation of LNAPLs and fractal dimension

The scatter diagram of fractal dimension D and the residual saturation S_R is shown in Fig. 5. It can be seen that the fractal dimension has a positive relationship with the residual saturation. Using the SPSS curve estimation model (curve estimation models in SPSS include Linear, Logarithm, Inverse, Quadratic, Power, Compound, S, Logistic, Growth, Exponent) for optimal fitting analysis (the same below), it was found that Quadratic is the best fit model to describe the relationship between the fractal dimension of the medium and the residual saturation of LNAPLs, which is written as:

$$S_R = 192.02D^2 - 890.73D + 1\,040.8 \quad (7)$$

The coefficient of determination R^2 reaches 0.779 9 and the R^2 of other models is between 0.420 3 and 0.458 6. Take the derivative of the curve and $D \approx 2.32$ is the turning point, where $S_R \approx 7.83$. That is, when $D \leqslant 2.32$, the higher the fractal dimension, the smaller the residual saturation, and two of them have a negative correlation. When $D \geqslant 2.32$, the higher the fractal dimension, the greater the residual saturation, and two of them have a positive correlation.

2.2.2 Relationship between fractal dimension and pore structure parameters

The scatter diagram of the pore structure parameters-fractal dimension of each medium is plot in Fig. 6, and the SPSS linear regression coefficient of determination R^2>0.36 was used as the criterion for judging the correlation. The results show that there

Table 3 Volume of samples and particle size

NO.	Volume (cm^3)			Accumulated in particle size $\frac{W}{W_0}$(%)						
	V_{soil}	V_{sand}	V_{oil}	0.03-0.3 mm	0.3-0.4 mm	0.4-0.5 mm	0.5-0.65 mm	0.65-0.8 mm	0.8-1 mm	1-2 mm
1-1	3 377.20	1 808.39	127.71	8.58	7.23	6.38	6.53	4.81	3.27	63.25
1-2	3 354.15	1 847.72	137.35	7.97	6.88	6.09	6.40	4.74	3.46	64.46
2-1	3 384.92	1 763.58	167.47	12.71	9.48	7.74	7.38	4.75	2.81	55.15
2-2	3 338.76	1 763.58	115.66	13.05	9.41	7.76	7.56	5.09	3.27	53.87
3-1	3 365.69	1 646.01	181.93	22.63	15.98	12.57	11.39	6.76	3.33	27.35
3-2	3 338.76	1 646.01	133.73	19.82	15.68	12.81	12.01	7.40	3.90	28.39
4-1	3 323.38	1 692.96	201.20	24.24	19.97	16.46	15.37	9.22	4.40	10.35
4-2	3 338.76	1 720.87	196.39	24.86	19.93	16.39	15.24	9.00	4.02	10.56

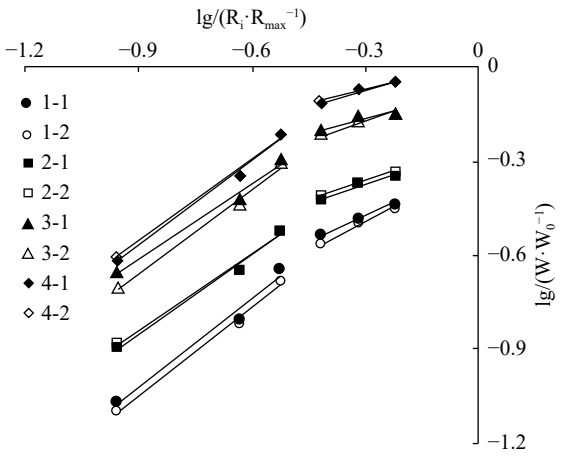

Fig. 4 The log-log plot of $lg(W/W_0)$ and $lg(R_i/R_{max})$ for each soil column

is a correlation between the fractal dimension of the medium and all pore structure parameters under the experimental conditions. Among them, the fractal dimension is positively correlated with fine sand content (R^2=0.785 3), porosity (R^2=0.725 4), and particle size variation coefficient (R^2=0.476 4). The fractal dimension of soil is negatively correlated with permeability coefficient (R^2=0.856 5), coarse sand content (R^2=0.828 1), and medium sand content (R^2=0.650 1).

2.2.3 Relationship between residual saturation and pore structure parameters

A scatter diagram of the pore structure parameters and residual saturation of each medium was plot in Fig. 7, and the coefficient of determination of SPSS linear regression R^2>0.36 was used as the criterion for judging the correlation. The results show that: Under the experimental conditions, the residual saturation of LNAPLS has no correlation with permeability coefficient (R^2=0.198 4) and porosity (R^2=0.096 8). However, it is positively correlated with the particle size variation coefficient (R^2=0.891 4) and fine sand (R^2=0.788 6), and negatively correlated with the content of medium sand (R^2=0.890 9) and coarse sand (R^2= 0.739 5).

2.3 Discussion

2.3.1 Significance of correlation

Both residual saturation and fractal dimension are controlled by the pore structure of the medium, which generally includes three parameters: Pore connectivity, pore size, and pore number (Lei et al. 2018). Based on the general law of pore structure law, this study mainly uses permeability coefficient to characterize pore connectivity. And low permeability coefficient mostly indicates low connectivity. Pore size can be reflected by the particle size and small particle size normally leads to small pores size and high porosity is related to a large number of pores. In addition, medium heterogeneity is another index of pore structure, which is characterized by the particle size variation coefficient in this experiment. High particle size variation coefficient may indicate strong heterogeneity.

Based on the above, the significance of the statistical relationship between the fractal dimension and residual saturation and each parameter are given in Table 5. Generally speaking, under the experimental conditions, smaller pore size indicates stronger heterogeneity in the medium higher fractal dimension and higher residual saturation. Larger numbers of pores are related to a poorer connectivity and higher fractal dimension, but the residual saturation does not change significantly.

Overall, pore size and heterogeneity are co-

Table 4 Key results

Treatment		1-1	1-2	2-1	2-2	3-1	3-2	4-1	4-2
	Line 1	2.44	2.41	2.59	2.55	2.73	2.69	2.71	2.73
D	Line 2	2.08	2.07	2.17	2.19	2.19	2.12	2.18	2.20
	Mean	2.26	2.24	2.38	2.37	2.46	2.41	2.45	2.47
S_R (%)Residual saturation		8.14	9.12	10.33	7.34	10.58	7.90	12.34	12.14
n_0 (%)Porosity		46.45	44.91	47.90	47.18	51.09	50.70	49.06	48.46
K(m/d)Permeability coefficient		79.16	50.85	41.91	61.36	27.35	39.82	37.04	46.51
$R_{Coarse-sand}$Coarse sand (%)		51.52		43.05		21.44		7.73	
$R_{Medium-sand}$Medium sand (%)		22.52		21.91		14.76		6.19	
$R_{Fine-sand}$Fine sand (%)		25.96		35.04		63.8		86.09	
RSD_{sand}RSD of sand content (%)		47.53		32.02		79.79		137.06	

NOTE: $RSD_{sand} = \frac{SDR_{Coarse-sand}, R_{Medium-sand}, R_{Fine-sand}}{AverageR_{Coarse-sand}, R_{Medium-sand}, R_{Fine-sand}} \times 100.$

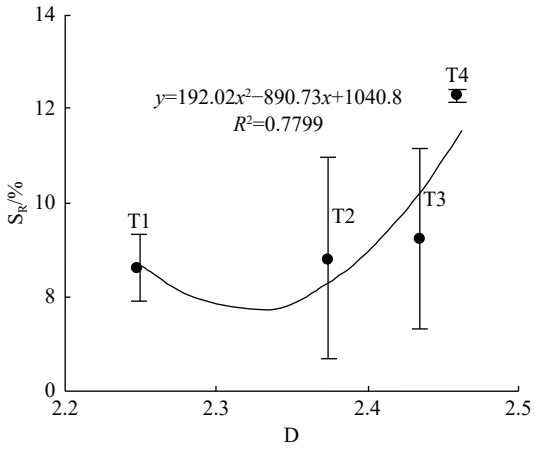

Fig. 5 The best fitting curve of D-SR

correlated parameters of fractal dimension and residual saturation.

2.3.2 Formation mechanism of LNAPLs fractal in sand medium

The fractal dimension is a comprehensive characterization of the structure of the entire medium pores (consisting of five types of pores: Connected pores, roars, dead pores, micro capillary pores and isolated pores) (Zhang et al. 2013; Han et al. 2018) (Fig. 8). The residual saturation of LNAPLS in sandy soil is theoretically controlled by the structure of micro capillary pores in the medium that can bind LNAPLs (Hayden et al. 2006; Cheng et al. 2014; Guo et al. 2014). Under the experimental conditions, it can explain the poor correlation between permeability coefficient (connected pores), porosity (total voids in the medium) and residual saturation. Because of this, the fractal dimension of the sand medium measured in this experiment is slightly different from the positive correlation between the fractal dimension and the LNAPLS residual saturation in the existing rock medium research results. However, the optimal fit of the regression model is a quadratic curve relationship, and the two are not strictly correlated.

2.3.3 The main controlling factors of the formation mechanism

Because the parameters of medium structure measured in the experiment actually have internal relationships with each other, such as: The permeability coefficient, which characterizes pore connectivity, is a combined reflection of other structural parameters; the content of coarse sand, medium sand and fine sand is negatively correlated, but the particle size variation coefficient and porosity are positively correlated with particle content. From a statistical point of view, only by eliminating the linear relationship between the parameters can the relationship between the independent variable and the dependent variable be truly reflected.

Therefore, SPSS multiple linear regression analysis was used in the study to establish the regression equations of fractal dimension, residual saturation and pore structure parameters of each medium (the coefficient of determination R^2 is all 1, and Sig. is all 0):

$$D = 2.844 \times std(R_{Fine-sand}) - 1.869 \times std(RSD_{sand}) - 0.270 \times std(n_0) \quad (8)$$

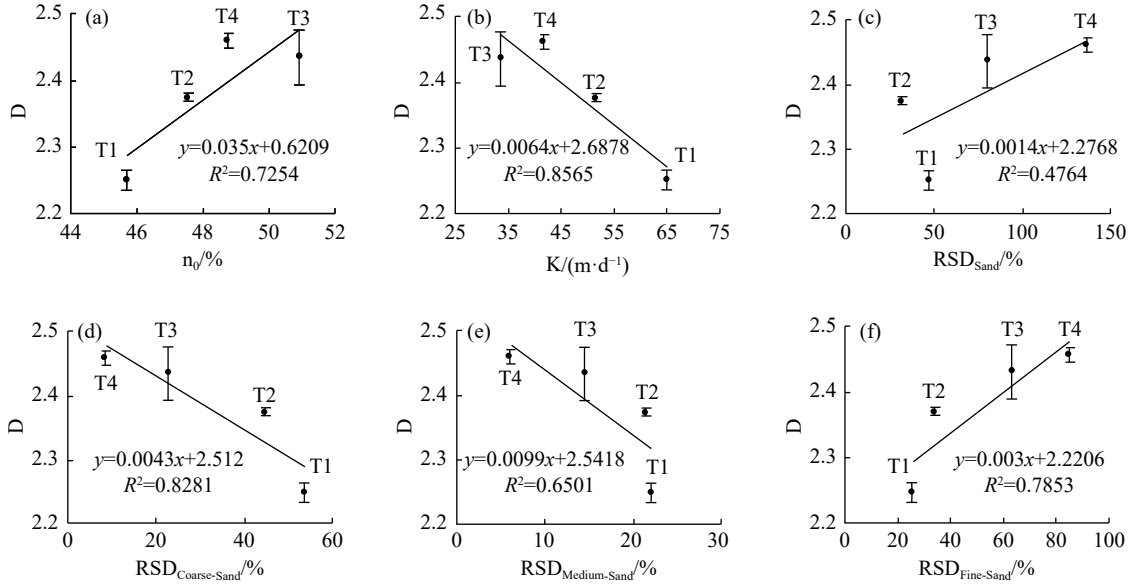

Fig. 6 Relationship between pore structure parameters and fractal dimension

NOTES: (a) porosity - fractal dimension, (b) permeability coefficient - fractal dimension, (c) particle size variation coefficient - fractal dimension, (d) coarse grain content - fractal dimension, (e) medium sand content - Fractal dimension, (f) fine sand content - fractal dimension

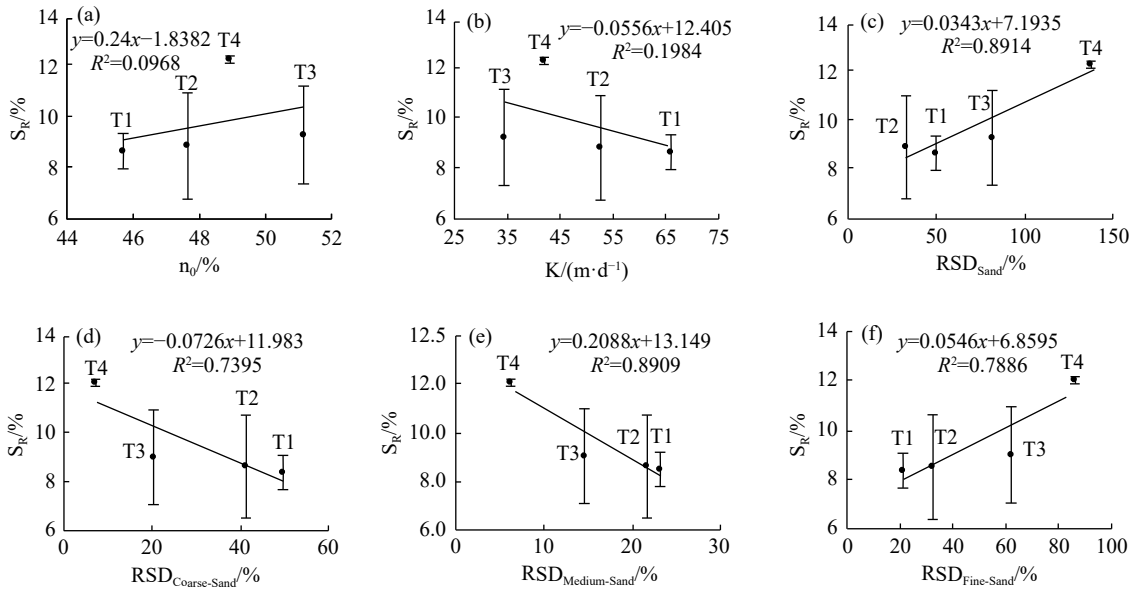

Fig. 7 Relationship between medium structure parameters and residual saturation of LNAPLs

NOTES: (a) porosity - residual saturation, (b) permeability coefficient - residual saturation, (c) particle size variation coefficient - residual saturation, (d) coarse grain content - residual saturation, (e) medium sand content - residual saturation, (f) fine sand content - residual saturation.

Table 5 Parameter relationship statistics and physical significance

Structural parameters	Fractal dimension	Residual saturation	Significance
Coarse sand content	Negative correlation	Negative correlation	The smaller the pores, the larger the fractal dimension and the larger the residual saturation
Medium sand content	Negative correlation	Negative correlation	The smaller the pores, the larger the fractal dimension and the larger the residual saturation
Fine sand content	Positive correlation	Positive correlation	The smaller the pores, the larger the fractal dimension and the larger the residual saturation
Coefficient of particle size variation	Positive correlation	Positive correlation	The stronger the heterogeneity, the larger the fractal dimension and the larger the residual saturation.
Porosity	Positive correlation	/	The more pores, the larger the fractal dimension, but the change of residual saturation is not obvious
Permeability coefficient	Negative correlation	/	The worse the pore connectivity is, the larger the fractal dimension is, but the residual saturation does not change significantly

NOTE: / means no relationship

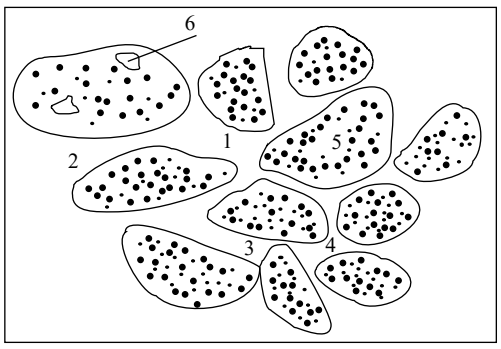

Fig. 8 Schematic diagram of pore structure of sand medium

NOTES: 1-connected pores, 2-roars, 3-dead pores, 4-microcapillary pores, 5-particles, 6-isolated pores

$$S_R = 1.944 \times std(R_{Fine-sand}) - 0.538 \times std(RSD_{sand}) - 0.844 \times std(n_0) \quad (9)$$

Where: *std* is the standardization of the scalar variable, which is calculated by the mean and standard deviation. It can be concluded that the fine sand content, the coefficient of variation of particle size, the particle size characterized by porosity, heterogeneity and the number of pores are the control factors of fractal dimension and residual saturation, among which the standard coefficient of fine sand content is the largest, therefore is regarded as the key control factor.

SPSS was used to analyze the optimal fitting between fine sand content and fractal dimension, and between fine sand content and residual saturation (Fig. 9), and the optimal fitting curves of the two were found to be in line with the quadratic model (R^2 was as high as 0.910 8 and 0.978 1):

$$D = 8 \times 10^{-5} \times R_{Fine-sand}{}^2 - 0.0121 \times R_{Fine-sand} + 2.0142 \quad (10)$$

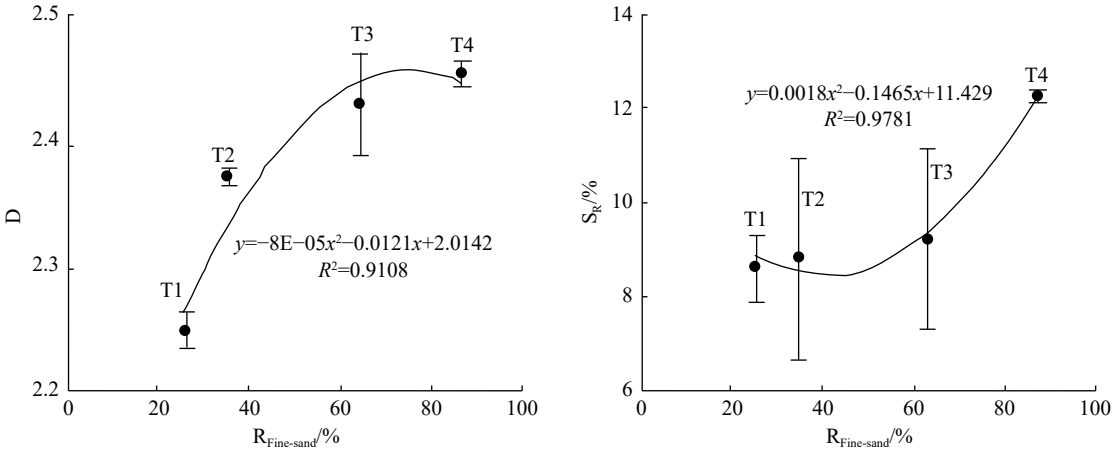

Fig. 9 The best fitting curve of fine sand content and D and SR

NOTES: (a) fine sand content - fractal dimension, (b) fine sand content - residual saturation

$$S_R = 1.8 \times 10^{-2} \times (R_{Fine-sand})^2 - 0.1465 \times R_{Fine-sand} + 11.429 \quad (11)$$

It can be seen that under the experimental conditions, the content of fine sand can almost be regarded as the main controlling factor of the fractal dimension of the medium, the residual saturation of LNAPLs, and the relationship between the two. The formation mechanism can be described as high content of fine sand is related to high probability of micro capillary pores and the LNAPLs are more easily to be bound. The effects of heterogeneity and pore number appear to be negligible.

It should be noted that in this experiment, the reason why this phenomenon is obvious is that the coarse, medium and fine sands are mixed uniformly in the mixing process and the overall homogeneity of the medium is good, and the particle variation coefficient that characterizes the heterogeneity RSD_{sand} is defined as the particle size function. However, in practical application, the heterogeneity of the medium, the numbers of pores, etc. are not solely controlled by the particle size. The general geometry, scale, continuity, porosity, permeability and heterogeneity caused by its spatial variation have a considerable impact on the residual saturation of LNAPLs. The fractal dimension is essentially a comprehensive characterization of the overall pore structure of the medium, and the fractal dimension of the medium is the most scientific, universal and convenient method to characterize the residual saturation of LNAPLs in theory.

3 Conclusions

In this study, statistical methods were used to characterize the relationship between the fractal dimension of sand media and the residual saturation of LNAPLs. Through the measurement and analysis of macro parameters of soil structure, the internal mechanism and main characteristics of this relationship were studied under the experimental conditions. The research can provide support for the assessment of residual LNAPLs in contaminated aquifers and the formulation of remediation measures in LNAPLs-contaminated aquifers. The main conclusions are as follows:

(1) The relationship between the fractal dimension of the sand medium and the residual saturation of LNAPLs was confirmed. The optimal fit satisfies the Quadratic model $S_R = 192.02D^2 - 890.73D + 1040.8$, and the coefficient of determination (R^2) reaches 0.779 9. (2) The statistical relationship between the fractal dimension of the sand medium, the residual saturation of LNAPLs and the pore structure parameters revealed that: Under the experimental conditions, smaller pore size is related to larger fractal dimension, and higher residual saturation; stronger heterogeneity is related to larger the fractal dimension and higher residual saturation. (3) The fine sand content can be considered as the main controlling factor of the relationship between the fractal dimension of the sand medium and the residual saturation of LNAPLs, which satisfies the Quadratic model.

Based on the above, it is expected that: (1) Similar research can be carried out in soils with smaller particles such as silt and clay and with more micro capillary pores, and in heterogeneous media with low-permeability lenses, which has a more profound significance for the remediation of LNAPLs pollution; (2) This study only conducted research on the macrostructure fractal of the pore and residual LNAPLs in the medium. By applying scanning electron microscopy, transmission electron microscopy, CT and other imaging techniques, microscopic pore structure of the medium

and the distribution characteristics of LNAPLs can be further investigated to achieve a better understanding. It is also expected that this research can provide a more scientific basis for the study of the "tailing" effect of NAPLs in porous aquifers and for the formulation of pollution remediation plans.

Acknowledgements

This research was financially supported by projects of the National Natural Science Foundation (No. 42007171), the Hebei Natural Science Foundation (No. D2021504034) .

References

Celia MA, Reeves PC, Ferrand LA. 1995. Recent advances in pore scale models for multiphase flow in porous media. Reviews of Geophysics, 33(S2): 1049-1057.

Cheng Y, Zhu J. 2021. Significance of mass–concentration relation on the contaminant source depletion in the nonaqueous phase liquid (NAPL) contaminated zone. Transport in Porous Media, 137(2): 399-416. (in Chinese)

Cheng Z, Wu JC, Xu HX, et al. 2014. Migration of DNAPL under the action of lens and surfactant. China Environmental Science, 34(11): 2888-2896. (in Chinese)

Costa A. 2006. Permeability - porosity relationship: A reexamination of the Kozeny - Carman equation based on a fractal pore - space geometry assumption. Geophysical research letters, 33(2): L02318.

Ezeh CG. 2019. Novel ideas for enhanced oil recovery and oil spill remediation in porous media. Tulane University School of Science and Engineering.

Feng XD, Zhang Y, Ma YF, et al. 2019. Research status of NAPLs seepage characteristics and models in porous media. Journal of Shandong University of Technology (Natural Science Edition), 33(04): 15-18+23. (in Chinese)

Forsyth PA, Shao BY. 1991. Numerical simulation of gas venting for NAPL site remediation. Advances in Water Resources, 14(6): 354-367.

Fetter CW, Boving TB, Kreamer DK. 1999. Contaminant hydrogeology. Upper Saddle River: Prentice hall: 178-218.

Gao F, Liu F, Chen H H. 2008. Research progress on remediation of trichloroethylene-contaminated soil and groundwater pollution source areas. Advances in Earth Science, 23(08): 39-47. (in Chinese)

Guo WM, Li ZP, Jia GL, et al. 2014. Quantitative interpretation of residual oil microdistribution and study on pore microstructure changes. Science Technology and Engineering(31): 32-36. (in Chinese)

Han H, Ding Z, Dong C, et al. 2018. Fractal characteristics of bulk-mudrock, washed, and kerogen samples of Chang 7 member mudrocks from the Ordos Basin, China. Journal of Petroleum Science and Engineering, 170: 592-606. (in Chinese)

Hayden N, Diebold J, Farrell C, et al. 2006. Characterization and removal of DNAPL from sand and clay layered media. Journal of Contaminant Hydrology, 86(1/2): 53-71.

Hou ZY, Wang Y, Lu WX. 2019. An alternative model for multiphase flow simulation for groundwater DNAPLs pollution remediation. China Environmental Science, 39(7): 2913-2920. (in Chinese)

Hunt JR, Sitar N, Udell KS. 1988. Nonaqueous phase liquid transport and cleanup: 1. Analysis of mechanisms. Water Resources Research, 24(8): 1247-1258.

Jia FS, Shen PP, Li KW. Fractal characteristics and application of sandstone pore structure. Fault Block Oil and Gas Field, 1995, 02(1): 16-21. (in Chinese).

Kacem M, Esrael D, Boeije CS, et al. 2019. Multiphase flow model for NAPL infiltration in both the unsaturated and saturated zones. Journal of Environmental Engineering, 145(11): 04019072.

Karaoglu AG, Copty NK, Akyol NH, et al. 2019. Experiments and sensitivity coefficients analysis for multiphase flow model calibration of enhanced DNAPL dissolution. Journal of contaminant hydrology, 225: 103515.

Kemblowski MW, Wen JC. 1993. Contaminant spreading in stratified soils with fractal permeability distribution. Water resources research, 29(2): 419-425.

Khasi S, Ramezanzadeh M, Ghazanfari MH. 2020. Experimentally based pore network modeling

of NAPL dissolution process in heterogeneous porous media. Journal of contaminant hydrology, 228: 103565.

Le YX, Wang CJ. 2004. Using fractal conditional simulation and streamline model to predict the distribution of remaining oil and gas saturation. Natural Gas Geoscience, 15(1): 42-46. (in Chinese)

Lei G, Mo S, Dong Z, et al. 2018. Theoretical and experimental study on stress-dependency of oil–water relative permeability in fractal porous media. Fractals, 26(02): 1840010. (in Chinese)

Li HY, Du XM, Yang B, et al. 2013. Capillary fingering morphology and fractal characterization of NAPLs fluids in porous media. Environmental Science (10): 334-341. (in Chinese)

Li ZF, He SL, Yang WX, et al. 2006. Microphysical simulation of water flooding experiment and research on fractal characteristics of residual oil distribution. Journal of China University of Petroleum (Natural Science Edition), (03): 75-79, 84. (in Chinese).

Liu HY, Tian ZY, Xu ZY. 2017. Quantitative evaluation of pore structure of carbonate reservoirs based on fractal characteristics. Lithologic Reservoirs, (5): 97-105. (in Chinese).

Mackay D, Shiu WY, Maijanen A, et al. 1991. Dissolution of non-aqueous phase liquids in groundwater. Journal of Contaminant Hydrology, 8(1): 23-42.

Mackay DM, Cherry JA. 1989. Groundwater contamination: pump-and-treat remediation. Environmental Science & Technology, 23(6): 630-636.

Mateas DJ, Tick GR, Carroll KC. 2017. In situ stabilization of NAPL contaminant source-zones as a remediation technique to reduce mass discharge and flux to groundwater. Journal of contaminant hydrology, 204: 40-56.

Mukhopadhyay S, Cushman JH. 1998. Diffusive transport of volatile pollutants in nonaqueous-phase liquid contaminated soil: A fractal model. Transport in porous media, 30(2): 125-154.

Neuman SP. 1995. On advective transport in fractal permeability and velocity fields. Water Resources Research, 31(6): 1455-1460.

Patmonoaji A, Muharrik M, Hu Y, et al. 2020. Three-dimensional fingering structures in immiscible flow at the crossover from viscous to capillary fingering. International Journal of Multiphase Flow, 122: 103147.

Ramezanzadeh M, Khasi S, Fatemi M, et al. 2020. Remediation of trapped DNAPL enhanced by SDS surfactant and silica nanoparticles in heterogeneous porous media: Experimental data and empirical models. Environmental Science and Pollution Research, 27(3): 2658-2669.

Rane K S, Goual L, Zhang B. 2020. Graphene wuantum dots for the mobilization and solubilization of nonaqueous phase liquids in natural porous media. ACS Applied Nano Materials, 3(11): 10691-10701.

Saripalli KP, Rao PSC, Annable MD. 1998. Determination of specific NAPL-water interfacial areas of residual NAPLs in porous media using the interfacial tracers technique. Journal of contaminant hydrology, 30(3-4): 375-391.

Soto MAA, Lenhard R, Chang HK, et al. 2019. Determination of specific LNAPL volumes in soils having a multimodal pore-size distribution. Journal of environmental management, 237: 576-584.

Wang X, Lanning LM, Ford RM. 2016. Enhanced retention of chemotactic bacteria in a pore network with residual NAPL contamination. Environmental science & technology, 50(1): 165-172.

White MD, Oostrom M, Lenhard RJ. 2004. A practical model for mobile, residual, and entrapped NAPL in water - wet porous media. Groundwater, 42(5): 734-746.

Wiedemeier, Todd H. 1999. Natural attenuation of fuels and chlorinated solvents in the subsurface. New York: John Wiley.

Yang K, Xu SY. 2009. Research on microscopic residual oil experimental method. Fault block oil and gas fields, 16(4). (in Chinese) Doi: CNKI: SUN: DKYT.0.2009-04-026.

Yu BM. 2003. Research progress on fractal analysis of transport properties in porous media. Advances in Mechanics, 33(3): 333-346. (in Chinese)

Zhang GH, Ren XJ. 2011. Fractal characteristics of pore structure in low-permeability reservoirs and its influence on water flooding efficiency.

Petroleum Geology and Oilfield Development in Daqing, 30(2): 94-99. (in Chinese)

Zhang FC, Kang SZ. 2007. Research progress on the migration of non-aqueous fluids in porous media. Journal of Soil Sciences(04): 170-177. (in Chinese)

Zhang XG, Zhang T, Lin CY. 2013. Pore structure evaluation of low permeability reservoirs based on pore fractal characteristics. Lithologic Reservoirs, 25(6): 40-45. (in Chinese)

Zhao YS, Han HH, Chi ZF, et al. 2018. Study on the effect of permeability difference on the migration of pollutants in low-permeability lenses. China Environmental Science, 38(12): 4559-4565. (in Chinese)